

The Influence of Pencil Graphite Hardness on Voltammetric Detection of Pentachlorophenol

Katarzyna Skrzypczyńska¹, Krzysztof Kuśmierk¹, Andrzej Świątkowski¹, Lidia Dąbek^{2,*}

¹ Institute of Chemistry, Military University of Technology, Kaliskiego 2, 00-908 Warsaw, Poland,

² Faculty of Environmental, Geomatic and Energy Engineering, Kielce University of Technology, al. Tysiąclecia Państwa Polskiego 7, 25-314 Kielce, Poland,

*E-mail: ldabek@tu.kielce.pl

Received: 8 July 2017 / Accepted: 8 September 2017 / Online Published: 1 December 2017

A pencil graphites were used for detection of pentachlorophenol (PCP) based on differential pulse voltammetry (DPV) and cyclic voltammetry (CV). The voltammetric studies were carried out using a pencil graphite electrode (GPE), carbon paste electrode (CPE) and powdered electrode (PE). The pencil graphites were characterized with scanning electron microscope (SEM), Raman spectroscopy and powder X-ray diffraction (XRD) methods. The effects of deposition potential, scan rate and pulse amplitude were examined to optimize the differential pulse voltammetry conditions. Compared to the other working electrodes the graphite pencil electrodes were recognized by their low cost, simplicity, commercial availability and ease of modification. The voltammetric studies have shown the usefulness of the pencil graphite as an electrode material. Their electrochemical usability increased with decreasing hardness (2B> 5B> 8B).

Keywords: graphite pencil electrode, carbon paste electrode, pentachlorophenol, voltammetric determination

1. INTRODUCTION

The use of carbon working electrode for the determination of organic compounds is steadily growing due to the good conductivity, long-term stability and low residual current. The best known carbonaceous electrodes are those involving glassy carbon, carbon paste, carbon fiber, screen-printed carbon strips, etc. [1-4]. Carbon paste is one of the most attractive material for electroanalysts [5-7] due to its easy surface recondition, easy modification and reproducibility.

Pentachlorophenol (PCP) has been commonly used as pesticide, wood preservative and disinfectant. As its overuse in the past, now it can be found in environment throughout the World Health Organization [8]. However, as a persistent organic contaminant with highly toxic, PCP is

carcinogenic and harmful to living organisms including humans [9]. Moreover, in tap water, the maximum admissible concentration of the pesticide has been strictly controlled to be trace level by European Union and the United States Environmental Protection Agency (0.5 and 1 $\mu\text{g L}^{-1}$, respectively) [10-13].

In recent years, several methods for the detection of pentachlorophenol have been described [14-22]. In this study, three types of the electrodes including pencil graphite electrode, carbon paste electrode modified with pencil graphite as well as powder electrode were prepared and used for the detection of pentachlorophenol. Three types of the pencil graphite with different hardness (2B, 5B and 8B) have been tested. Graphite is the most important component of pencil lead - in fact, it's actually made up of a mixture of graphite and clay. The composition of this mixture determines its hardness grade. The higher the proportion of graphite content relative to clay the lead has, the softer and darker the lead will be. The European scale was coined by the KOH-I-NOOR in the Czech Republic. This system uses a combination of letters and numbers. The "B" symbol denotes soft leads or leads with a greater graphite content. The higher corresponding number, the softer the lead and the darker the marks produced by the lead. The "H" symbol designates leads with the higher clay content.

Recently, graphite pencil electrodes were used for the detection and determination of many environmental contaminants including metal ions [23-26], inorganic pollutants [27-29], phenolic compound [30-31], organic dyes [32] and pesticides [33-34]. However, the graphite pencil electrodes were not compared with other electrodes. To our best knowledge, the electrochemical detection of the pentachlorophenol at the different electrodes based on pencil graphite have not been reported so far [35]. In this study the electrochemical characteristics and behavior of the produced pencil graphite electrodes were examined by cyclic and different pulse voltammetry. Physical characterization of the electrodes was done with Raman and X-ray diffraction methods. The SEM images were taken to investigate the morphology of the electrodes used.

2. EXPERIMENTAL

2.1. Chemicals

The pentachlorophenol was received from Merck. The pencil graphites were purchased from KOH-I-NOOR (Hardtmuth a.s., Czech Republic). The graphite powder (45 μm), spectroscopic grade mineral oil (Nujol) and potassium ferricyanide were purchased from Sigma Aldrich (St. Louis, USA).

The voltammetric experiments were carried out in 0.1 mol L^{-1} sodium sulfate. The solutions were prepared with doubly distilled water. Nitrogen gas (MULTAX S.A.) was passed over the solutions during all of the voltammetry measurements. The ethanol (96%), hydrochloric acid (35%), potassium chloride and sodium sulfate were from POCh (Gliwice, Poland).

2.2. Electrochemical studies

Cyclic voltammetry (CV) and differential pulse voltammetry (DPV) measurements were performed in AutoLab (Eco Chemie, the Netherlands), potentiostat PGSTAT 20 connected to a three

electrode cell. A conventional three-electrode cell assembly was used. The reference electrode was a saturated calomel electrode and the counter electrode was a platinum wire. The working electrode was either a graphite pencil electrode, modified carbon paste electrode or a powder electrode. The system was run on a PC using GPES 4.9 software. Before each analysis, the working electrode was polished with alumina to 0.2 μm thickness, followed by cleaning in an ultrasonic bath in water for 5 min and thorough rinsing with distilled water. The cyclic voltammetry measurements were operated with a potential range from -1.0 to +1.0 V and a scan rate of 50 mV s^{-1} . The CV measurements were performed in potential range from -0.5 V to +1.45 V with the scan rate as 50 mV s^{-1} in a redox probe solution of 2 mmol L^{-1} $\text{Fe}(\text{CN})_6^{3-}/\text{Fe}(\text{CN})_6^{4-}$ (1:1) prepared in 0.1 mol L^{-1} KCl.

2.3. Pencil graphite characterization

The X-ray diffraction powder analysis (XRD) was performed to identify the phases using BRUKER D8 Discover diffractometer equipped with a standard Cu $K\alpha$ radiator ($\lambda = 1.54056 \text{ \AA}$, Siemens KFL CU 2 K, 40 kV voltage and 40 mA current in operating mode). The Bragg-Brentano geometry diffraction for 2θ range 10-60 was used. The step size was equal to 0.015, acquisition time was 2 seconds per step and $T = 298 \text{ K}$. Measurements of the chemical compositions were carried out using Philips XL30/LaB6 scanning microscope coupled with an energy dispersive X-ray spectrometer (EDS). The characterization of the pencil graphite was done by Raman spectroscopy using Renishaw inVia Raman Microscope with 785 nm excitation wavelength.

For a more complete characterization of the pencil graphites their adsorption capacities towards pentachlorophenol were also tested. The adsorption experiments were carried out in a batch mode with the following procedure. A 10 mL of the PCP solutions (from 1.0 to 10.0 mg L^{-1}) were added to an Erlenmeyer flasks containing the same amounts of the pencil graphites (0.5 g). The mixtures were agitated for a predetermined period of time (4 h) at 200 rpm. At the expiration of this period, the mixtures were filtered through a 0.2 μm pore size filter and analyzed by high-performance liquid chromatography method described elsewhere [36]. The equilibrium amount of PCP adsorbed per unit mass of the graphite, q_e (mg g^{-1}), was calculated by the following equation:

$$q_e = \frac{(C_0 - C_e)V}{m} \quad (1)$$

where C_0 and C_e are the initial concentration and equilibrium concentration of the PCP (mg L^{-1}), V is the volume of the solution (L) and m is the mass of the adsorbent (g).

2.4. Preparation of the electrodes

In these studies three types of working electrodes including the pencils graphite of different hardness, the modified carbon paste electrode and the powder electrode were used.

The first type of working electrode was constructed with 2B, 5B or 8B graphite leads (PGE/2B, PGE/5B and PGE/8B). The posterior end of the pencil lead was connected to a copper wire of electrical contact. The pencil lead was tightly coated with Teflon band and its tip was polished on a

smooth paper to a smoothed finish. During the measurements the 1.5 cm of the graphite lead was introduced into the solution to be analyzed while the holder was kept in the upright position.

The second type of working electrode was carbon paste electrode modified with graphite pencil (CPE/2B, CPE/5B and CPE/8B). An ideal paste electrode should exhibit good electroanalytical ability. The CPE was prepared by mixing graphite powder and paraffin oil. The paste was incorporated into the electrode cavity and polished with alumina to 0.2 μm thickness. The modified CPE was initially prepared by mixing graphite powder (90%, *m/m*) and one type of the pencil graphite (2B, 5B or 8B) and subsequently adding mineral oil. The mixture was pounded in a mortar for at least 10 min to produce the final (homogenous) paste and kept at 25°C for 48 h. Next, the paste was packed into the electrode cavity (2.5 mm) with \varnothing 3.5 mm. The electrode surface could be renewed by simple extraction of a small amount of paste from the tip of the electrode.

The last type of working electrode was powder electrode (PE/2B, PE/5B and PE/8B). The powdered material was placed in an electrode container and immersed with a solution to obtain a sedimentation layer. All potentials were measured and are reported against a potassium chloride saturated calomel electrode (SCE) connected to the electrochemical cell *via* an agar-agar/KCl bridge. A Pt wire was served as the counter electrode. The analyses were carried out in potential ranges preventing the electrochemical modification of the surface of the materials used.

3. RESULT AND DISCUSSION

3.1. Characterization of the pencil graphite

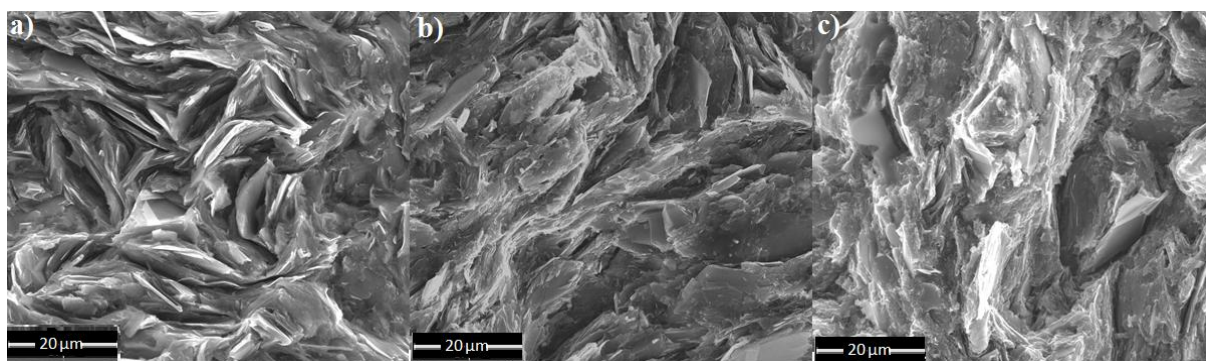


Figure 1. The SEM images of the 2B (a), 5B (b) and 8B (c) pencil graphites.

The morphologies of the pencil graphite were investigated using scanning electron microscopy (SEM). The SEM images are shown in Fig. 1. Since electrochemistry is based fundamentally on the interfacial phenomena, the nature of the electrode surface is of importance. It is evident that the roughness of the electrodes is related to the granularity of the conductive materials. The pencil graphite is characterized by a surface formed by irregularly shaped micrometer sized flakes of graphite.

The EDS analysis of the pencil graphite was shown in Table 1. The pencil graphites contain of graphite and kaolin. As shown in the Table 1, the carbon content (graphite) decreases as the pencil

graphite hardness increases. All of the samples tested can also find small amounts of other elements such as potassium, calcium, titanium and iron.

Table 1. Chemical composition (wt. %) of investigated pencil graphites measured by EDX.

Element	2B	5B	8B
	Wt. %	Wt. %	Wt. %
C	59.23	69.16	75.08
O	20.72	14.78	13.79
Si	9.13	7.43	5.26
Al	7.54	5.85	4.00
K	0.75	0.49	0.25
Ca	0.26	0.24	0.26
Mg	0.18	0.19	0.28
Ti	0.37	0.16	0.30
Fe	1.82	0.80	1.24

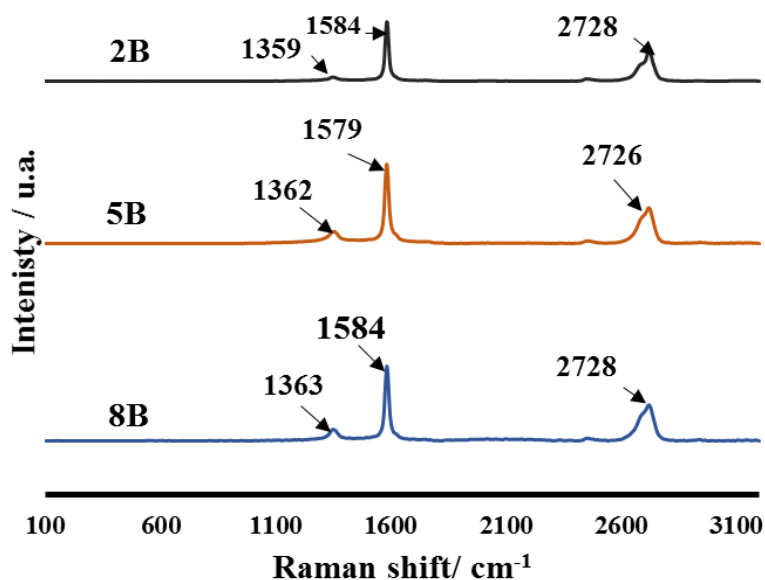


Figure 2. Raman spectra of the G, D and 2D bands for 2B, 5B and 8B pencil graphites.

The Raman spectroscopy is a useful method for the characterization of graphite-based materials. Figure 2 shows the Raman spectra of 2B, 5B and 8B pencil graphites. Although G, 2D and D bands were observed for each electrode, the intensities and peak maximums had different values. The D bands of the pencil graphite were determined to be 1359, 1362 and 1363 cm^{-1} for PGE/2B, PGE/5B and PGE/8B, respectively. The G bands were identical for pencil graphites 2B, 5B and 8B (1584 cm^{-1}).

The position of the 2D bands was comparable for each electrodes. The peak ratio of I_G/I_D were 0.158, 0.149 and 0.072 for the pencil graphites 2B, 5B and 8B, respectively.

The pencil graphite for hardness 2B, 5B and 8B were characterized with X-ray diffraction method (Fig. 3).

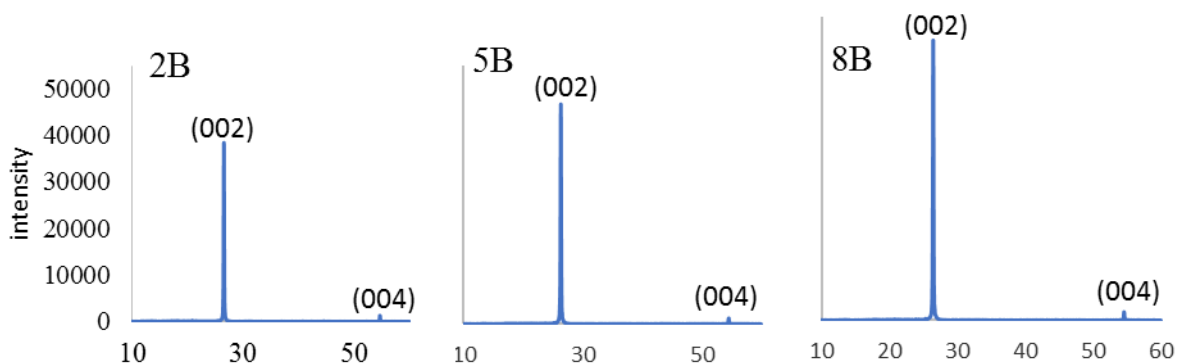


Figure 3. The XRD analysis of the pencil lead.

The result shows only the (002) and the (004) peaks of graphite, which is a sign that the pencil lead is made of natural graphite [35]. This explains the various impurities present in the sample. The average size of the graphite grains were estimated using the “Scherrer formula” [37]:

$$D = \frac{0.9 \lambda}{B \cos \theta} \tag{2}$$

where D is the average grain size, λ is the wavelength of the X-ray used in the measurement =1.54056 Å, B is the full-width at half-maximum width of the XRD peak, and θ is the Bragg angle of the peak. Using Eq. 2 and the results presented in Fig. 3, the average size of the graphite grains was found to be approximately 154 nm.

3.2. Adsorptive properties of the pencil graphites

The adsorption isotherms of the PCP on the pencil graphites as well as on the commercial Sigma-Aldrich graphite are presented in Fig. 4. The adsorption equilibrium data were fitted using the Langmuir and Freundlich isotherm models [38]. The Langmuir isotherm is employed to monolayer adsorption while the Freundlich isotherm is widely applied for adsorption surfaces with nonuniform energy distribution. The equations of the isotherms can be represented as follows:

Langmuir model

$$q_e = \frac{q_{mL} K_L C_e}{1 + K_L C_e} \tag{3}$$

Freundlich model

$$q_e = K_F C_e^{1/n} \tag{4}$$

where: q_m [mg g^{-1}] is the maximum adsorption capacity, K_L [L mg^{-1}] is the Langmuir constant related to the free energy of the adsorption, K_F [$(\text{mg g}^{-1}) \cdot (\text{L mg}^{-1})^{1/n}$] is the Freundlich equation constant which relate to the adsorption capacity, and n is the adsorption intensity of the adsorbent. All of the model parameters were evaluated by non-linear regression using the OriginPro 7.5 software. The calculated adsorption constants and the correlation coefficients are presented in Table 2.

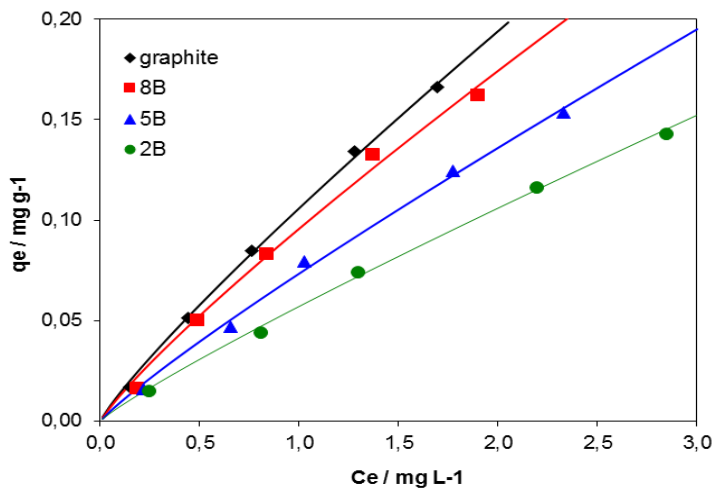


Figure 4. Adsorption isotherms of the PCP on the pencil graphites.

Table 2. Parameters of the Langmuir and Freundlich isotherm models for the adsorption of PCP on the graphites

Graphite	Langmuir			Freundlich		
	q_m [mg g^{-1}]	K_L [L mg^{-1}]	R^2	K_F [$(\text{mg g}^{-1}) \cdot (\text{L mg}^{-1})^{1/n}$]	n	R^2
Sigma-Aldrich	0.767	0.164	0.993	0.106	1.370	0.998
Pencil 8B	0.664	0.173	0.992	0.096	1.160	0.997
Pencil 5B	0.512	0.158	0.991	0.074	1.127	0.996
Pencil 2B	0.405	0.151	0.991	0.057	1.119	0.998

The regression correlation coefficient values show that the equilibrium data obtained were well represented by both models, nevertheless, a higher R^2 values (≥ 0.996) were observed for the Freundlich equation. The values of the Freundlich constant K_F as well as the Langmuir maximum adsorption capacity (q_m) increased in the order: $2B < 5B < 8B < \text{Sigma-Aldrich}$ graphite. The adsorption capacity of the pencil graphites is much lower than activated carbons [39,40]. This is not surprising, since their specific surface area is tens of times greater than the graphite. However, the adsorption of the PCP is comparable or greater than the other low porous materials including eggshell

($K_F = 0.028 \text{ (mg g}^{-1}) \cdot (\text{L mg}^{-1})^{1/n}$) [38], spent mushroom compost ($K_F = 0.056$) [41] or almond shell ($K_F = 0.075$) [42].

3.3. Voltammetry

3.3.1. Optimization

For the purpose of determining the electroactive surface area of all of the electrodes the electrochemical behaviour of potassium ferrocyanide in 1 mol L^{-1} KCl supporting electrolyte was studied. The CV voltammogram of 1.0 mmol L^{-1} $\text{K}_3[\text{Fe}(\text{CN})_6]$ in 0.1 mol L^{-1} KCl recorded at the same scan rates is presented in Fig. 5.

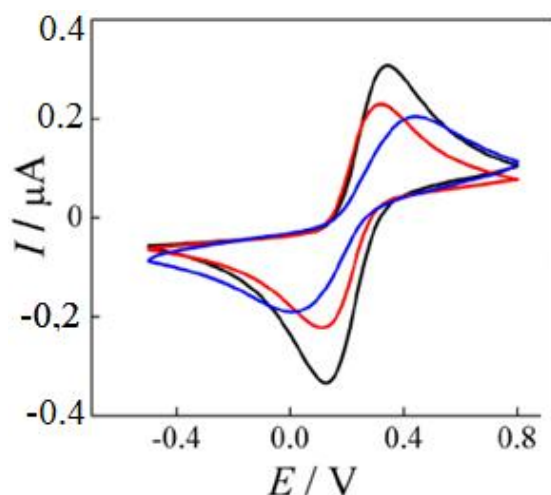


Figure 5. Cyclic voltammogram of 1.0 mmol L^{-1} potassium ferrocyanide in 0.1 mol L^{-1} KCl recorded on PGE/8B (black line), PGE/5B (red line) and PGE/2B (blue line).

The peak current for a reversible process is described by the Randles-Sevcik equation (5):

$$I_p = 2.69 \times 10^5 A D^{1/2} n^{3/2} v^{1/2} C \quad (5)$$

where: A is area of the electrode (cm^2), n is the number of electrons participating in the reaction (equal to 1), D is the diffusion coefficient of the molecule in solution, C is the concentration of the probe molecule in the solution (2 mmol L^{-1}) and v is the scan rate (V s^{-1}).

Based on the results presented in Fig. 5 the value of the active electrode area was found to be 0.198 cm^2 for all of the electrodes.

The effects of the scan rates (from 10 mV s^{-1} to 100 mV s^{-1}) on the peak potential and the pentachlorophenol peak current were evaluated. The anodic peak current increased with increasing scan rate. For the whole range of the scan rates studied, the peak shape shows irreversible characteristics. The anodic current recorded at about $+0.79 \text{ V vs. SCE}$ increased linearly with the $v^{1/2}$

(as shown in Fig. 6) indicating a mass-transfer controlled process. Optimization for carbon paste electrodes was described elsewhere [43].

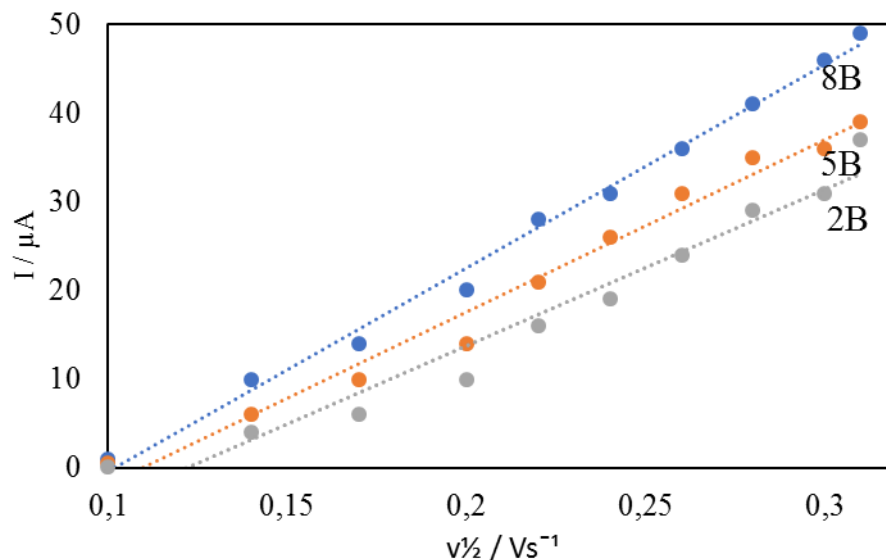


Figure 6. Plot of I_{pa} versus $v^{1/2}$ for the oxidation of pentachlorophenol at pencil graphite electrode for different hardness: 8B, 5B and 2B.

The values of the R^2 for the anodic peaks current versus $v^{1/2}$ were 0.96; 0.98 and 0.99 (expected about 1.0) for the 2B, 5B and 8B pencil graphite electrodes, respectively. The logarithm of the peak current vs. logarithm of the scan rate suggested that the oxidation process is predominantly diffusion-controlled (Fig. 6).

3.3.2. Effect of modifier content

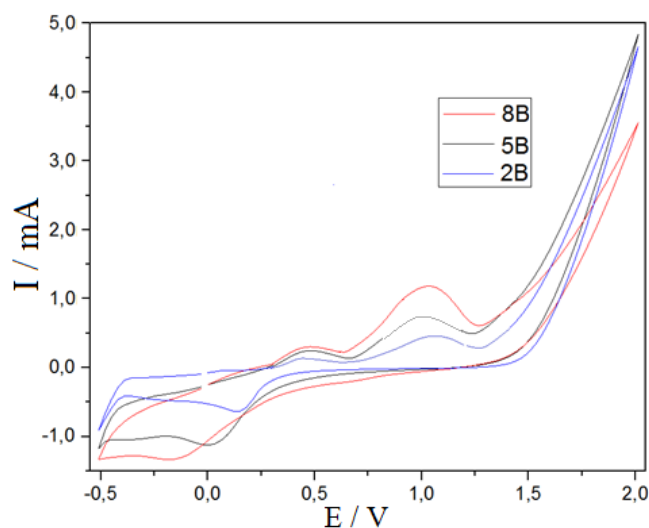


Figure 7. Cyclic voltammogram pencil graphite electrode for different hardness: 8B, 5B and 2B recorded in 0.5 mmol L^{-1} PCP.

The CV was used to develop a voltammetric methodology for the detection and determination of the PCP in water samples. Cyclic voltammogram for all of the PGEs are shown in Fig. 7.

The oxidation process of the pentachlorophenol on the pencil graphite electrodes occurred at the potential value of approximately +0.99 V versus SCE, and only one peak appeared. The current corresponding to the peak oxidation of PCP increased with increase in the graphite content (2B<5B<8B). On the reverse scan from +2.0 V to -0.5 V vs. SCE, no corresponding reduction peak was observed within the potential range between +2.0 and +0.40 V vs. SCE, revealing that the anodic PCP oxidation on the PGE electrode was totally irreversible. The same test was performed for the powder electrodes and carbon paste electrodes modified with the same materials.

3.3.3. Analytical application

The linearity of the methods was tested in the pentachlorophenol concentrations from 0.1 to 0.5 mmol L⁻¹. The calibration curves were obtained by plotting the peak current vs. the PCP concentration. The characteristics of the calibration plots are presented in Table 3. The limits of detection (LOD) and quantification (LOQ) were calculated from the calibration curves as $3\sigma/a$ and $6\sigma/a$, respectively, where: a is a slope of the calibration curve and σ is a standard deviation of the blank signal. As can be seen, all of the calibration curves for PCP measurements were linear in the studied ranges (the R^2 values were more than 0.98).

Table 3. Linearity results for the pencil graphite electrodes

Analytical method	Linear regression equation $y = ax + b$	R^2	LOD [mmol L ⁻¹]	LOQ [mmol L ⁻¹]
PGE/2B	$y = 0.76x + 0.038$	0.997	0.277	0.554
PGE/5B	$y = 1.11x + 0.048$	0.985	0.189	0.379
PGE/8B	$y = 2.15x + 0.070$	0.989	0.098	0.195
CPE/2B	$y = 3.40x + 0.274$	0.992	0.097	0.194
CPE/5B	$y = 4.24x + 0.405$	0.983	0.078	0.156
CPE/8B	$y = 5.76x + 0.541$	0.996	0.057	0.114
PE/2B	$y = 0.67x + 0.066$	0.985	0.179	0.358
PE/5B	$y = 0.87x + 0.082$	0.956	0.137	0.277
PE/8B	$y = 1.28x + 0.059$	0.987	0.090	0.186

The sensitivity of the electrodes was correlated with the hardness of the pencil graphites (2B < 5B < 8B). The best results were observed for the 8B pencil graphite for all of the tested electrodes. Carbon paste electrodes were found to be better than the PGE and PE electrodes. The LOD and LOQ observed for the CPE modified with the 8B pencil graphite was 0.057 and 0.114 mmol L⁻¹, respectively. Comparison of different electrodes for electrochemical detection of PCP is presented in Table 4.

The LOD of the pencil graphite based electrodes was much more worse than other electrochemical methods [17-24]. However, these electrodes, as cheap and not requiring additional preparation, can be used for the preliminary detection of pentachlorophenol.

Table 4. Sensitivity of the different electrodes used for detection of PCP.

Electrode	LOD [mol L ⁻¹]	References
CPE/8B	5.7×10^{-5}	this study
glassy carbon electrode	4.5×10^{-5}	[17]
multi-wall carbon nanotubes-epoxy composite electrode	1.6×10^{-6}	[18]
glassy carbon electrode surface with CuS nanocomposites and chitosan	6.2×10^{-7}	[19]
chitosan modified carbon paste electrode	4.0×10^{-7}	[20]
Pt/ZnO/AChE/chitosan bioelectrode	5.3×10^{-8}	[21]
nano-TiO ₂ -dihexadecylphosphate film modified electrode	1.0×10^{-8}	[22]
poly(Rhodamine B)/graphene oxide/multiwalled carbon nanotubes modified glass carbon electrode	5.0×10^{-10}	[13]
Ceria nanospheres modified platinum electrode	3.0×10^{-11}	[14]

The practical application of the pencil graphite electrodes was investigated for the determination of PCP in Vistula river water. The river water samples were spiked with different amounts of PCP with known concentrations (0.1 mmol L⁻¹) and analyzed without any pretreatment after the addition of 0.1 mol L⁻¹ sodium sulfate. The results (Table 5) demonstrates the good agreement of the added and found concentrations of the PCP. The recovery values were from 96.3 to 105.0% with the relative standard deviation (RSD) below 7.5%.

Table 5. Results of PCP determination in spiked river water samples.

Electrode	Added [mmol L ⁻¹]	Found [mmol L ⁻¹]	RSD [%]	Recovery [%]
PGE/2B	0.1	0.103±0.0076	7.4	103.3
PGE/5B		0.105±0.0056	5.3	105.0
PGE/8B		0.104±0.0046	4.4	104.0
CPE/2B		0.099±0.0045	4.5	99.3
CPE/5B		0.101±0.0046	4.5	101.0
CPE/8B		0.100±0.0025	2.5	99.7
PE/2B		0.104±0.0042	4.0	103.7
PE/5B		0.096±0.0032	3.3	96.3
PE/8B		0.105±0.0025	2.4	104.7

4. CONCLUSION

In this paper a three type of the electrodes containing pencil graphite with different hardness (2B, 5B and 8B) have been compared. The pencil graphite were characterized with SEM, Raman spectroscopy and XRD methods. For a more complete characterization of the pencil graphite their adsorption capacities towards pentachlorophenol were also tested. The influence of the instrumental parameters including the accumulation time and the scan rate were examined. The results showed that

the peak current increased with the decreasing hardness (2B > 5B > 8B). The results demonstrated that the pencil graphite electrode exhibited better electroanalytical performance and higher sensitivity toward PCP than the powder electrodes.

ACKNOWLEDGEMENTS

The work was partially supported by RMN 08-788. The authors are grateful to MSc Sylwia Cieślak for technical assistance by SEM-EDS measurements.

References

1. B. Uslu, S.A. Ozkan, *Anal. Let.*, 40 (2007) 817-853.
2. I. Svancara, K. Vytras, K. Kalcher, A. Walcarus, J. Wang, *Electroanalysis*, 21(2009) 7-28.
3. K. Wasiński, P. Nowicki, P. Pórolniczak, M. Walkowiak, R. Pietrzak, *Int. J. Electrochem. Sci.*, 12 (2017) 128-143.
4. V.K. Gupta, H. Mahmoody, F. Karim, I.S. Agarwal, M. Abbasghorbani, *Int. J. Electrochem. Sci.*, 12 (2017) 248-257.
5. M. Mazloum-Ardakani, H. Rajabi, H. Beitollahi, B.B.F. Mirjalili, A. Akbari, N. Taghavinia, *Int. J. Electrochem. Sci.*, 5 (2010) 147-157.
6. J. Guo, Y. Luo, F. Ge, Y. Ding, J. Fei, *Microchim. Acta*, 172 (2011) 387-393.
7. H.S. El-Desouky, M.M. Ghoneim, *Talanta*, 84 (2011) 223-234.
8. U.G. Ahlborg, T. Hunberg, *Crit. Rev. Toxicol.*, 7 (1980) 1-35.
9. B. Xia, , Y. Qiming, C. Mingfu, W. Shaofei, G. Rui, Y. Shanli, L. Chengbin, L. Shenglia, *Sensors and Actuators B Chemical*, 2016, 565-572.
10. H.A. Hattemer-Frey, C.C. Travis, *Arch. Environ. Contam. Toxicol.*, 18 (1989) 482-489.
11. P.G. Jorens, P. J. Schepens, *Hum. Exp. Toxicol.*, 6 (1993) 479-495.
12. Toxic Substance Control Act U.S. Environmental Protection Agency, Washington, D.C (1979).
13. N. Nesakumar, M. B. Gumpu, S. Nagarajan, S. Ramanujam, J. Bosco, B. Rayappan, *Measurement* 109 (2017) 130–136g
14. X. Zhu, K. Zhang, N.Lu, X. Yuan, *Applied Surface Science*, 361 (2016) 72–79
15. A. Jakab, *Desalin. Water Treat.*, 52 (2014) 1462-1471.
16. A.N. Kawde, N. Baig, M. Sajid, *RSC Adv.*, 6 (2016) 91325-91340.
17. A. Remes, A. Pop, F. Manea, A. Baci, S.J. Picken, J. Schoonman, *Sensors*, 12 (2012) 7033-7046.
18. E.C. Guijaro, P. Yanez-Sedeno, J.M. Pingarron Carrazon, L.M. Polo Diez, *Analyst.*, 113 (1988) 625-62
19. Y. Wu, *Sensors and Actuators B*, 137 (2009) 180–184
20. J. Xu, Y. Wang, H. Qiu, Y. Zhang, *Russian Journal of Electrochemistry*, 2014, 531–536
21. J. Zou , J. Ma , Y. Zhang , L.Li , J. Jiang, J. Chen, *Analytical Letters*, 46:7 (2013) 1108-1116
22. N. Nesakumar, S.Sethuraman, U. M. Krishnan, *J. Appl. Electrochem.*, 46 (2016) 309–322
23. G. Flora, D. Gupta, A. Tiwari, *Interdiscip. Toxicol.*, 5 (2012) 47-58.
24. M.K. Ali, R. Ansari, A.F. Delavar, Z. Mosayebzadeh, *Bull. Korean. Chem. Soc.* 33 (2012) 1247-1252.
25. R. Ansari, A.F. Delavar, A. Mohammad-Khah, *J. Solid State Electrochem.*, 9 (2014) 5092-5115.
26. M. Abdul Aziz, A. N. Kawde, *Talanta*, 115 (2013) 214-221.
27. B.E. Watt, A.T. Proudfoot, A. Vale, *Toxicol. Rev.*, 23 (2004) 51-57.
28. N. Kawde, M.A. Aziz, N. Baig, Y. Temerk, *J. Electroanal. Chem.*, 720 (2015) 68-74.
29. A. Ozcan, *Electroanalysis*, 26 (2014) 1631-1639.
30. I.G. David, I.A. Badea, G.L. Radu, *Turk. J. Chem.* 37 (2013) 91-100.

31. A. Ensafi, B. Rezaei, M. Amini, E. Heydari-Bafrooei, *Talanta*, 88 (2012) 244-251.
32. Y. Yardin, E. Keskin, A. Levent, M. Ozsoz, Z. Senturk, *Talanta*, 80 (2010) 1347-1355.
33. E. Keskin, Y. Yardin, Z. Senturk, *Electroanalysis*, 22 (2010) 1191-1199.
34. K. Kuśmierk, P. Idźkiewicz, A. Świątkowski, L. Dąbek, *Arch. Environ. Prot.*, 43 (2017) DOI: 10.1515/aep-2017-0029
35. I. G. David, *Anal. Methods*, 8 (2016) 6537-6544.
36. G. Sun, X. Li, Y. Qu, X. Wang, H. Yan, Y. Zhang, *Mater. Lett.*, 62 (2008) 703- 706.
37. O. Hamdaoui, E. Naffrechoux, *J. Hazard. Mater.*, 147 (2007) 381-394.
38. W. Abdel Salam, R.C. Burk, *Water Air Soil Poll.*, 210 (2010) 101-111.
39. N.T. Abdel-Ghani, G.A. El-Chaghaby, E.M. Zahran, *Int. J. Environ. Sci. Technol.*, 12 (2015) 211-222.
40. W.M. Law, W.N. Lau, K.L. Lo, L.M. Wai, S.W. Chiu, *Chemosphere*, 52 (2003) 1531-1537.
41. B.N. Estevinho, N. Ratola, A. Alves, L. Santos, *J. Hazard. Mater.*, B137 (2006) 1175-1181.
42. X. H. Xie, X. J. Li, H.H. Yan, *Mater. Lett.*, 60 (2006) 3149-3152.
43. K. Skrzypczyńska, K. Kuśmierk, A. Świątkowski, *J. Electroanal. Chem.*, 766 (2016) 8-15.

© 2018 The Authors. Published by ESG (www.electrochemsci.org). This article is an open access article distributed under the terms and conditions of the Creative Commons Attribution license (<http://creativecommons.org/licenses/by/4.0/>).